# Nuclear Decay Rate Oscillations and a Gravity-Quantum Connection

Robert T. Longo*
rtlongo370@gmail.com

January 16, 2019

**Abstract**

This paper construct a model to evaluate the hypothesis that the incompatibility between General Relativity and Quantum Mechanics is due to the different space-time geometries upon which each respective theory was built. The model is then applied to an unexplained phenomena observed in the decay rate of unstable nuclei, whose decay rate has superimposed on them oscillations that match the yearly cycle of the Earth's orbit. The gravity-quantum connection model will show that gravitation is likely the "*unknown field*" responsible for the nuclear decay oscillations.

keyword: gravitation; quantum systems; radioactivity oscillations; alpha decay; beta decay.

## 1 Introduction

The genesis of this paper was to build a model to test the hypothesis that the different space time geometries of General Relativity (GR) and Quantum Mechanics (QM), as well as all classical physics, are responsible for the incompatibility of these theories. It became clear the model could offer a yet to be conceived explanation for the phenomena of a yearly oscillation observed in nuclear decay rates. Attending to this dual purpose, this paper is divided into two parts. Part I develops the model and discusses the connection between GR and QM. Part II the model is applied to the nuclear decay oscillation phenomena.

---

*PhD in Physics and a Technical Fellow Boeing Aircraft Company, retired

## 2   Part I

### 2.1   The Model

It is well known that a connection between GR and QM has not been found. Both GR and QM in their realm are superior theories but do not work well together. The general trend of theoretical physics is to quantize gravitation in the hope this will solve the problem. In this model we will take a different approach: The underlying philosophy to connect GR and QM is to use the inherit difference of the definition of space and time. GR is based upon a non-Euclidean geometry where space and time are merged into space-time following Minkowski [1]. Gravitation emerges due to the inclusion of energy. QM, is built in space and time defined by Newton and is based upon Euclidean geometry. Special Relativity takes the speed of light to be constant and adds observers in relative motion. This alters the measurements of space and time as seen by different observers; however, their descriptive physics are built in Euclidian geometry of Newtonian space and time. In our present paradigm, a materialistic philosophy of the world is held, we believe GR to be the proper spacetime, and all material object must reside in the GR spacetime [2].
Fields are important and fundamental entities in our present physics, and are thought to be two layered [3]. The first layer is a mathematical abstraction and cannot be measured or manipulated. The field quantities are used in the second layer to define measurable entities. The concept of abstract fields is important in the model that is built here.

### 2.2   Rules of the Model

From here on, *Newton space and time* will be referred to as (NST) and Einstein General Relativity as *Einstein spacetime* (EST). An abstract field $\sigma^\mu$ is defined for each coordinate by a comparison of the two space time geometries and has consequences at only one $EST$ point where real physical interaction occurs. It is given by

$$\sigma \equiv \frac{Geometry \; of NST}{Geometry \; of EST} \tag{1}$$

.

The $\sigma$ field is applied to classical, or quantum, coordinates by replacing all $NST$, coordinate by $\sigma^\mu x^\mu$ thus pulling classical coordinates onto the $EST$ manifold. The $\sigma$ field is valid at only one point in $EST$ and carries $EST$ information at its origin to other locations. There are several ways to

define $\sigma$; Using the ratio of the line elements of each geometry or, using the equations of motion. For this paper the equations of motion will be used because they introduce an added constraints important in Part II. It will be assumed, for this work, that all fields are static and isotropic. The equations of motion [4] are given by

$$\frac{d^2 x_E^\mu}{d\tau^2} + \Gamma_{E\alpha\beta}^\mu \left(\frac{dx_E^\alpha}{d\tau}\right)\left(\frac{dx_E^\beta}{d\tau}\right) = 0, \tag{2}$$

in $EST$ and $\tau$ is the proper time[1]. The equivalent equation of motion in $NST$ are obtained by working backwards from Newtons gravity

$$\frac{d^2 \mathbf{x}_N}{dt^2} = -\nabla \Phi. \tag{3}$$

Where $\mathbf{x}_N$ are spacial coordinates. Further and converting from coordinate time to proper time, gives

$$\frac{d^2 \mathbf{x}_N}{d\tau^2} = \frac{1}{2}\left(\frac{dt_N}{d\tau}\right)^2 \nabla h_{tt} = 0. \tag{4}$$

Where $h_{tt}$ is a small quantity, defined by $g_{\mu\nu} = \eta_{\mu\nu} + h_{\mu\nu}$ and $\nabla h_{tt} = \frac{\partial h_{tt}}{\partial x_N^\alpha}$ and $\Gamma_{Ntt}^\alpha = -\frac{1}{2}\eta^{\alpha\beta}\frac{\partial h_{tt}}{\partial x_N^\alpha}$. The acceleration of coordinate time is

$$\frac{d^2 t_N}{d\tau^2} = 0. \tag{5}$$

This finally gives the final $NST$ equations of motion in a similar form to the equation of motion in EST.

$$\frac{d^2 x_N^\mu}{d\tau^2} + \Gamma_{Ntt}^\mu \left(\frac{dt_N}{d\tau}\right)^2 = 0. \tag{6}$$

A four component field $\sigma^\mu$ will be defined as the first integral of each geometric coordinate. The first integrals are constants of motion, energy and angular momentum, thus $\sigma's$ are constants with respect to proper time. However, position and velocity may change, but will be dependent on each other and the constants of motion. The components of $\sigma$ will change the scale of the $NST$ physics. $\sigma's$ are only defined at one point, where a physical interaction occurs, thus all derivatives of $\sigma$ are zero. We assume the Schwarzschild solution, in $EST$, because we are interested in relatively local physics.

---

[1]The coordinate labels N or E refers to the geometry that defines them. They will be dropped later.

The components of the equations of motion in $EST$ are

$$0 = \frac{d^2r}{d\tau^2} + \frac{A'(r)}{2A(r)}(\frac{dr}{d\tau})^2 - \frac{r}{A(r)}(\frac{d\phi}{d\tau})^2 + c^2\frac{B'(r)}{2A(r)}(\frac{dt}{d\tau})^2 \qquad (7)$$

$$0 = \frac{d^2\theta}{d\tau^2} \qquad (8)$$

$$0 = \frac{d^2\phi}{d\tau^2} + \frac{2}{r}(\frac{d\phi}{d\tau})(\frac{dr}{d\tau}) \qquad (9)$$

$$0 = \frac{d^2t}{d\tau^2} + \frac{B'(r)}{B(r)}(\frac{dt}{d\tau})(\frac{dr}{d\tau}) \qquad (10)$$

where $A(r) = (1 - R_s/r)^{-1}$, $B(r) = (1 - R_s/r)$ and $R_s = 2GM/c^2$, and $\theta = \pi/2$. The first integral of Eqs. (7-10) are

$$0 = A(r)c^2(\frac{1}{c^2}(\frac{dr}{d\tau})^2 + \frac{J^2}{A(r)c^2r^2} - 1 \qquad (11)$$

$$0 = \frac{d\theta}{d\tau} - constant \qquad (12)$$

$$0 = r^2\frac{d\phi}{d\tau} - J \qquad (13)$$

$$0 = \frac{dt}{d\tau} - \frac{1}{B(r)} \qquad (14)$$

The constants of motion are the energy per unit mass, $E$ and angular momentum per unit mass, $J$.

The equations of motion for $r$, $\theta$, $\phi$ and $t$ in the $NST$ geometry are

$$0 = \frac{d^2r}{d\tau^2} + \Gamma^r_{tt}(\frac{dt}{d\tau})^2 \qquad (15)$$

$$0 = \frac{d^2\theta}{d\tau^2} \qquad (16)$$

$$0 = \frac{d^2\phi}{d\tau^2} \qquad (17)$$

$$0 = \frac{d^2t}{d\tau^2} \qquad (18)$$

The first integral of Eqs. (15-18) are

$$0 = Kc^2(\frac{1}{c^2}(\frac{dr}{d\tau})^2 - 1) \tag{19}$$

$$0 = \frac{d\theta}{d\tau} - constant \tag{20}$$

$$0 = r^2\frac{d\phi}{d\tau} - J \tag{21}$$

$$0 = \frac{dt}{d\tau} - K \tag{22}$$

Now construct the $\sigma's$ for each coordinate using the prescription defined in Eq. (1). For $\sigma^\theta$ we choose the constants in both $EST$ and $NST$ to be the same. Similarly for $\sigma^\phi$ the angular momentum is the same in both geometries. The four $\sigma's$ for each coordinate are then

$$\sigma^r = K(1 - \frac{R_s}{r})(\frac{(1 - \frac{1}{c^2}((\frac{dr}{d\tau})^2) + \frac{J^2}{r^2})}{1 - \frac{1}{c^2}((\frac{dr}{d\tau})^2 - (1 - \frac{R_s}{r})\frac{J^2}{r^2})}) \tag{23}$$

$$\sigma^\theta = 1 \tag{24}$$

$$\sigma^\phi = 1 \tag{25}$$

$$\sigma^t = K(1 - \frac{R_s}{r}) \tag{26}$$

Eq. (23) requires some explanation: if we are describing the same phenomena in both $EST$ and $NST$, such as gravitational orbits, then the right hand factor in Eq. (23) will be close to one. On the other hand, if a high energy quantum effect is described in a relatively slow astronomical body then $\sigma^r$ will approach, but never reach, zero.

## 2.3 The EST and NST Geometries are Connected at a Point

To build this model further the NST space and time must be defined. The existing paradigm holds that all physical object exist only on the $EST$ space-time manifold [2], off the manifold no objects exist. This model envisions the $NST$ space and time geometry is built at a single point of the manifold where an interaction between material objects occur as a tangent space to the GR manifold and we imagine it exists only as long as the field it generates is free from other interactions. Further, imagined interactions do not share tangent spaces, each interaction has its own unique tangent space.

Tangent spaces are well defined, but do not exist physically they are abstract mathematical constructs. They exist only in our theory[2]. We further imagine, a tangent space comes into existence instantly when we imagine a physical interaction. It occurs and fills the entire universe instantly without regard to the speed of light. For quantum objects, they are the space where quantum probability amplitude fields, wave functions, exists. There is nothing a analyst must do except solve the quantum problem that includes the $\sigma$ field, in the appropriate variables. The wave function may vary in space and time in the $NST$ and carries with it a measure of the gravitational field at the creation point. The wave function in $NST$ is a ghost image of the physical object that moves in $EST$, restricted by the speed of light to another spacetime point where it enters into another interaction. The analyst must determine where the originating tangent space overlaps the $EST\ manifold$ point where the second interaction takes place. There the analyst will select the ghost wave function at that point to continue with the calculation. The original tangent space then becomes irrelevant and cannot be used in any further calculations. A second tangent space is instantly created at the new interaction point, again carrying a ghost wave function along with the $\sigma$ of that point.

## 2.4  Determining the Tangent space

To determine the tangent space at a point on a $EST$ manifold the GR solution can be embedded in a higher dimensional Euclidean space,[2] and [6]. Suppose the Schwarzchild manifold is the GR solution. Further suppose our interest is the radial direction. For simplicity we use the Misner embedding,[3] suppose our focus is on a quantum object located at a $EST$ point $(r_P, \theta_P, \phi_P, t_P)$. The embedding space function, $Z(r)$ is given by

$$Z(r_P) = (8\frac{GM}{c^2}(r_P - 2\frac{GM}{c^2}))^{1/2} + constant. \tag{27}$$

The slope of what will be called the tangent space x-axis, directionally aligned with the $EST$ r radial direction, is

$$\frac{dZ(r_P)}{dr} = (\frac{(2\frac{GM}{c^2 r_P})}{1 - 2\frac{GM}{c^2 r_P}})^{1/2}. \tag{28}$$

---

[2]This implicitly assumes that at a basic level, conscious living beings are necessary observers [5].

[3]Misner, etal Gravitation, see figure 23.1 on p614 and the discussion for the space out side a star

6

The 4-dimensional tangent space that represents the $NST$ is built around the tangent and normal to the manifold. The time axis is perpendicular to the other three. Figure1 shows a cut through the $NST$ tangent space showing the x-axis and the normal, or z-axis. The tangent is defined by the equation

$$\frac{dZ(r_P)}{dr}(x - r_P) + Z(r_P). \tag{29}$$
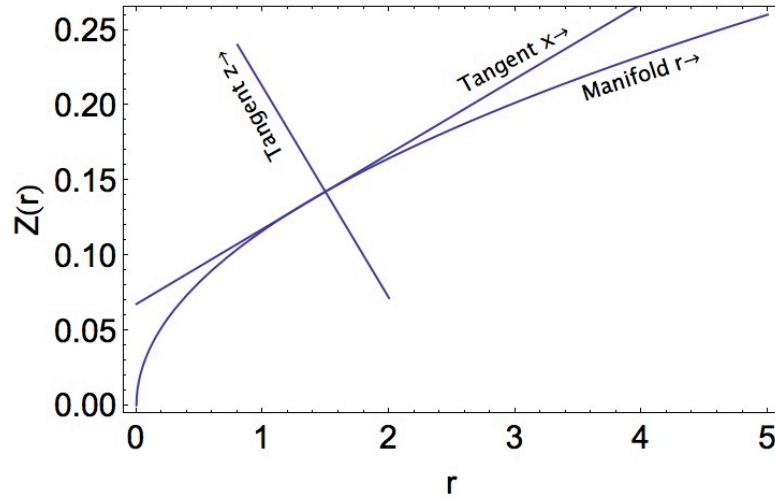


Figure 1: Shows a 2-dimensional slice through the x-axis of the tangent space and normal to the manifold.

It is assumed that a quantum ghost object spreads out spherically from its origination point in the tangent space and carries with it the gravitational field of the creation point as well as frequency, time and phase, and all relevant quantum states. Also, it exists as long as it does not interact with other quantum objects. When the real material quantum object, restricted to the $EST$ manifold and by the speed of light, reaches an intercept point the analyst must determine the position of the ghost object that coincides with the $EST$ point. This can be done by a transformation.

## 2.5 Tangent Space transformation

To describe the rules for locating the ghost quantum wave function in the tangent space, whch is intercepted at a distant point $Q$ on the manifold the

7

wave function $\Psi$ must be determined by finding the $EST$ point $(x_Q, z_Q)$ in the tangent space. This transformation is done by considering the Euclidean embedding space where vectors can be defined, see figure 2.
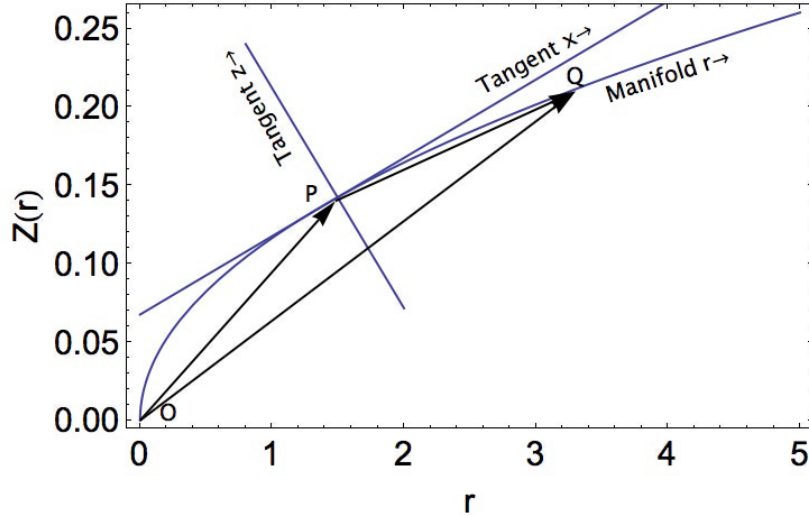


Figure 2: Shows a 2-dimensional slice through the x-axis, and normal of the tangent space to the embedded manifold. The vector $PQ$ is determined by the vector difference $OQ - OP$

To locate the tangent space point, in the case depicted in figure 2, that coincides with point $Q$ in $EST$, rotate the tangent space around the y-axis of the original point $P$, the y-axis points into the plane of the figure, until the tangent x-axis lies along the vector $PQ$ and coincides with point $Q$. Let $\alpha$ be the rotation angle and all point (x,z) in the tangent plane will transform as

$$x' = cos(\alpha)x + sin(\alpha)z, \tag{30}$$

$$z' = -sin(\alpha)x + cos(\alpha)z. \tag{31}$$

Where $x'$ lies along the rotated x-axis and $z' = 0$ using Eq. (31) the rotation angle can be found.

$$\alpha = \tan^{-1}(\frac{z}{x}). \tag{32}$$

Then $x'$ becomes

$$x' = cos(\tan^{-1}(\frac{z}{x}))(1 + (\frac{z}{x})^2)x. \tag{33}$$

The tangent coordinates at the point $Q$ in $EST$ are obtained by rotating the point $(x', 0)$ back to its original angle. The final tangent coordinates called $(x'', z'')$ are given by

$$x'' = cos(\tan^{-1}(\frac{z}{x}))^2(1 + (\frac{z}{x})^2)x, \tag{34}$$

$$z'' = sin(\tan^{-1}(\frac{z}{x}))cos(\tan^{-1}(\frac{z}{x}))(1 + (\frac{z}{x})^2)x. \tag{35}$$

The ghost wave function containing $(x'', z'')$ are used for the next calculation at point $Q$, to define measurable properties.

Tangent spaces always exist, for example for a given interaction a tangent space comes into existence and exist until the interaction that generated it undergoes another interaction at a different $EST$ location. Then that tangent space can no longer be used and a new tangent space is created at the same instant. Since all this is an abstraction its "creation" and "annihilation" are simply a choice of a conscious analyst. As a further complication, every quantum interaction in the universe creates a unique tangent space, so there can be infinite unique tangent spaces in existence at the same "$time$" but only those that interest a conscious observer are importance. We Imagine the universe filled with a multitude of tangent spaces coming and going, analogous to virtual particles.

The way to visualize this process is to take an example: consider the emission of a photon by some interaction happening to a real atom in $EST$. At that instant a tangent space is created and fills the universe and a ghost photon described by the wave function populates the entire tangent space at the same instant. The wave function is dynamic in the sense that it can vary with $NST$ space and time in the tangent space. All wave function dynamics are instantaneous and exists every where in the tangent space universe at the instant of creation, this is acceptable because the tangent space is not physical, its a mathematical abstraction.

From the moment the photon is created, the real materialistic photon propagates at the speed of light to a point where it interacts with another atom, and the process repeats itself. If for example, the second interaction is the detector of a telescope, then the ghost wave function is used. Suppose an analyst is calculating a quantum matrix element the result will have two $\sigma$ values in the result. For example, the wave function at the initial creation

9

point is $\Psi_n = e^{ik_n\sigma_1^r r}$ and at the final point the wave function is $\Psi_m = e^{ik_m\sigma_2^r r}$ then the matrix element will be

$$\langle\Psi_n^*|\Psi_m\rangle \Rightarrow \int_{-\infty}^{\infty} e^{+i(k_n\sigma_1^r - k_m\sigma_2^r)r}d^3r. \tag{36}$$

Where $\sigma_1^r$ is the $\sigma$ field where the photon was created and $\sigma_2^r$ is the $\sigma$ field where the photon was observed. This then injects the difference in gravitational field into the quantum calculation, the result gives $k_{n,m} = (k_n\sigma_1^r - k_m\sigma_2^r)$, thus a frequency shift will be observed where none was expected. This will have no effect on "table top" experiments, because to a high accuracy $\sigma_1^r = \sigma_2^r$ and they will be absorbed into the wave numbers. It is possible to ask about the wave function that represents the ghost photon but it is not possible to change anything or do any experiment on the ghost photon in its tangent space.

# 3 Part II

## 3.1 Observed Nuclear Decay Rates Anomalies

Nuclear decay rates have been studied from the late 1800's and are important to basic physics as well as science in general, such as material dating and medicine . Nuclear decay measurements have been studied with various external influences, such as temperature and pressure, looking for correlations but, none have been found [7]. Many unstable nuclei have long half lives and this has led experimenters to run measurements over extended periods to improve the accuracy of half life and test the longevity of measurement equipment. In turn many have observed a periodic oscillation, there have been about 23 such experiments, see [8]. Jenkins was the first to suggest the oscillations were influenced by unknown solar mechanisms due to the Earths orbit [9]. Long term measurements have been carried out by the Brookhaven National Laboratory (BNL) [10] between 1982 through 1986 . A longer test from 1984 to 1999 was run by [11] at the Physikalish-Technische Bundesandstalt (PTB). Both these observers witnessed the yearly oscillation. Both the BNL and PTB observations peak near the perihelion of the Earths orbit, but are shifted a few months from perihelion. On December 13, 2006 Jenkins [12] observed an anomaly in the decay rate of $^{54}$Mn coincident with a solar flair reported by GOES-11 X-ray data[13].
Evidence Against the influence of the Sun-Earth distance on nuclear decay was given by [14]. Norton's work does not show the oscillations and thus does not support the hypothesis discussed here, however a reanalysis of

Nortons data by [8] showed a weak yearly oscillation. If the effect is related to the distance of the experiment to the Sun then a space craft experiment should also see the effect, P. S. Cooper [15] analyzed the Cassini space craft RTG power source over a two year period and found no effect. The major difference between the Cassini data and the other observation is the shielding effect of the Earth's atmosphere, since $X-rays$ and $\gamma-rays$ will not penetrate the Earths atmosphere, but in space the intensity of these energetic photons may mask the weak gravitational effect.

## 3.2 A Test of this Model

The model developed in Part I shows that the unknown field from the Sun, suggested by Jenkins [9], is gravitation. The yearly cycles in the data, correlated with the elliptical orbit of the Earth, does not determine a gravitational effect and eliminate emissions from the Sun. To eliminate Sun emissions, finer details is examined to remove the Sun's influence. The yearly peaks in the decay rate of the PTB data are shown as dots in figure 3, and are connected by the solid line linking them. These peaks are measured from the normalized line at 1.000 as shown by the dashed vertical lines. The Earths elliptical orbit no longer has any influence, since each point is at the same place in the Earth's orbit with respect to the Sun. The model will shows that this fine structure is correlated with the position of the planets.
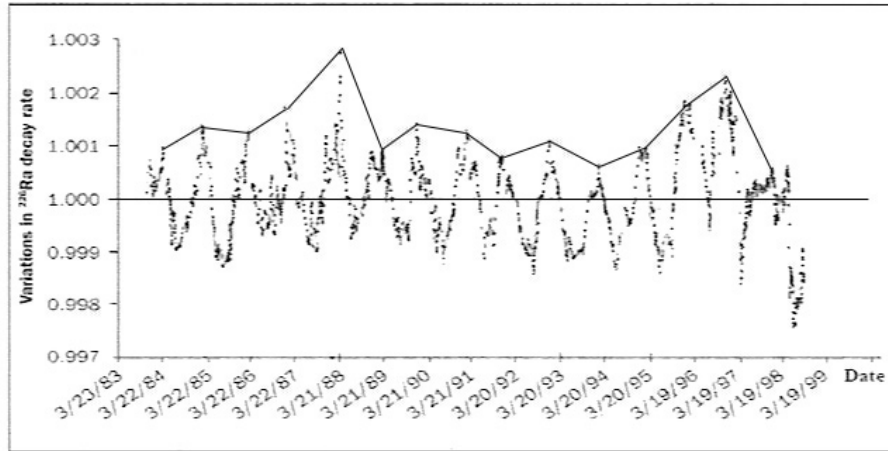


Figure 3: PTB data can be seen in [16] and [8]. Two distinct, increased count rate, peaks are seen in years near 1988 and 1997. The date scale starts on March 22,1984 and end on March 19, 1999

11

### 3.3 Counting Theory Modified by the Model

The standard theory for determining the half life of an unstable nuclei is

$$N(t) = N_0 e^{-\lambda t} \tag{37}$$

where $N(t)$ is the number of unstable nuclei remaining after a time $t$ has passed from the start of the measurements, and $N_0$ is the number of unstable nuclei at the start of the measurement. A normalize curve is obtained by multiplying each data point by $e^{-\lambda t}$ where $\lambda$ is the accepted decay rate given by $\lambda = ln(2)/t_{1/2}$ and $t_{1/2} = 1577 \pm 9 \ yr$ for the system of interest, $^{226}$Ra . Replacing $t$ by $\sigma^t t$ per the rules of the model, then using Eq. (26) gives

$$\frac{N(t)}{N_0} = e^{-\lambda \sigma^t t} = e^{-\lambda' t (1 - \frac{R_s}{r(t)})} \tag{38}$$

Where $\lambda' = K\lambda$, and $R_s/r = \sum_{i=1}^{n} R_{s_i}/r_i$ and $n$ is the number of planet and $r_i$ is the distance from the $i^{th}$ planet to the Earth. Then multiplying both sides of Eq. (38) by $e^{+\lambda' t}$ gives

$$\frac{N(t)}{N_0} e^{+\lambda' t} = e^{+\lambda' t (\frac{R_s}{r(t)})} \tag{39}$$

Taking the log of both sides and dividing by $\lambda' t$, then to first order in the gravitational field gives the result that will be studied for the planets position with respect to the Nuclear decay data.

$$k \frac{1}{\lambda' t} (ln(\frac{N(t)}{N_0} e^{+\lambda' t})) = \frac{R_s}{r}. \tag{40}$$

From Eq. (40) the gravitational effect on the Earth is the potential $R_s/r$ for all the influencing bodies up to a scaling factor $k$. Thus the quantum effect (LHS) is directly equal to the gravity effect (RHS)[4]. Since the (RHS) is a description of Gravitational effect, time is expressed as the proper time, whereas the (LHS) is a quantum effect, measured typically in coordinate time, the (LHS) must be converted to proper time.
This adds two new constants $K$ and $\kappa$, from Eq. (22), $t = \kappa \ \tau + K$ this will shift the relative time between the nuclear decay data and the astronomical calculations, and explain the shift of the decay data from the perihelion of the Earth's orbit, as observed. The values used in the calculations are $\kappa = 0.952$ and $K = 1490$.

---

[4]The normalization function $(N(t)/N_0)e^{+\lambda t}$ normally unity yields zero for the logarithm. In this case the rate $\lambda$ is modified by the $\sigma$ field, thus $(N(t)/N_0)e^{+\lambda' t}$ is not unity.

The way to interpret this, using the model is; every decay event creates a new tangent space and $\sigma$, that quickly becomes irrelevant when the quantum object is detected by the nearby detector, thus each decay is associated with a slightly different $r$ as the Earth and planets move.

## 3.4 Connecting the model to Astronomical events

To connect the model to the real world, the influence of the planets on the earth is determined. Only Venus and Jupiter, at the peak of each year are used[5]. To determined a planet's orientation we employed an online astronomical program [17]. The Earth and Sun remain in a fixed orientation each year at the peak of March 22, selected by the PTB experimenters.

## 3.5 Orbits of Venus and Jupiter and their Influence on Earth

The solar orbits of the planets are obtained using Kepler's law[6]. The radius from the Sun to the $i^{th}$ planets given by

$$r_i(t) = \frac{L_i^2}{GM_i}(1 + \epsilon_i cos(\omega_i t + \phi_i))^{-1}, \tag{41}$$

where $L_i$ is the orbital angular momentum, $M_i$ is the planets mass, $\epsilon_i$ is the eccentricity of the orbit, $\omega_i$ the angular frequency and $\phi_i$ the position of the planet at time zero. The distance from the Earth to the $i^{th}$ planet is

$$r_{1i}(t) = (r_1(t)^2 + r_i(t)^2 - 2r_1(t)r_i(t)cos(\omega_i t + \phi_i))^{1/2}. \tag{42}$$

The Contribution to the gravitational potential at the Earth $(i = 1)$ from the $i^{th}$ planet is obtained from the gravitational force[7]

$$\mathbf{F}_{1i}(t) = \frac{GM_iM_1}{r_{1i}(t)^2}\widehat{\mathbf{r}}_i(t). \tag{43}$$

Potential is normally obtained from the gravitational force by $V(r) = -\int_{\infty}^{\mathbf{r}} \mathbf{F}(\mathbf{r}) \cdot d\mathbf{r}$, which assumes that $r$ is an independent variable. In this case $r$ is not independent but dependent on time and is constrained to elliptical orbit. The potential in this case is taken to be

---

[5]All planets of the solar system were studied, all but Venus and Jupiter had a minor effect and were not further considered.

[6]The variables in Kepler's law do not need the inclusion of the $\sigma's$ since GR gives the same results, so the planetary orbits are part of $EST$.

[7]This clearly mixes the $NST$ and $EST$ theories, it is assumed to first order this is acceptable.

$$\Phi(t) = -\sum_{i=1}^{N} \int_{0}^{t} \mathbf{F}_i(\mathbf{r}_i(t)) \cdot \frac{d\mathbf{r}_i(t)}{dt} dt. \qquad (44)$$

Where $d\mathbf{r}_i(t)/dt$ is the radial, not orbital, velocity. In the case considered here, $N = 2$. The calculated results are shown in figure 4. The two peaks, near 1988 and 1997 are clearly represented by the model.
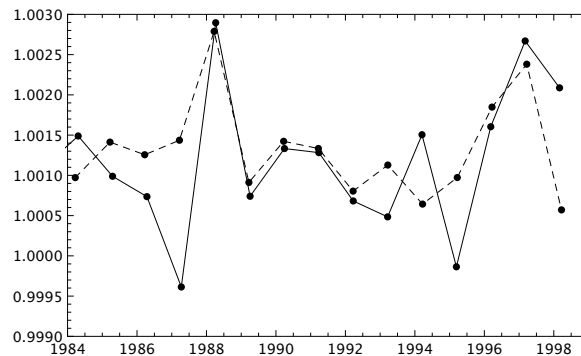


Figure 4: The yearly peaks in the PTB data discussed in Figure 3 are shown here as the dotted line. The solid curve is calculated by the model.

A check on the multi-body orbit calculation is made by measurements of the Planet to Earth distance each year using the astronomical program [17], where the physical dimensions are determined from the Sun to Earth, $1AU$, as indicated in Figure 5.

14
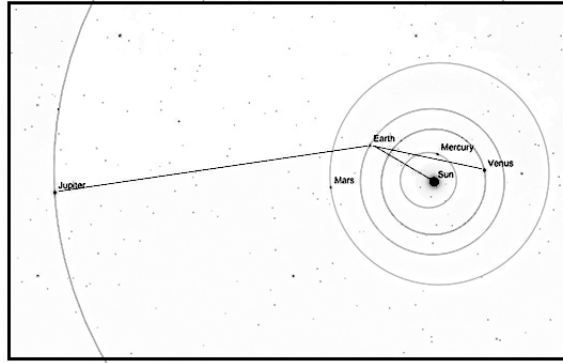
Figure 5: Shown here are the orbits for an arbitrary date. The Planet to Earth distances in units of AU are obtained from direct measurements, using SkySafari 6 Pro orbit graphics.

Results for each year are shown in Figure 6. Clearly the two main peaks are observable and consistent with the results shown in Figure 4.
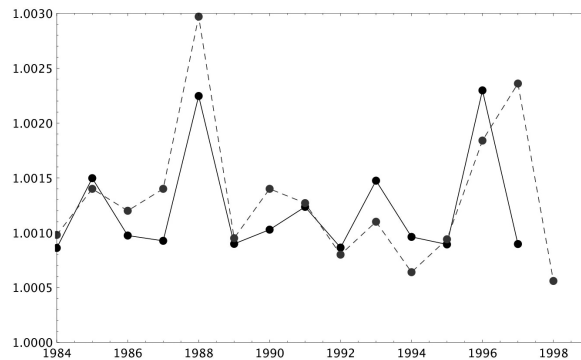


Figure 6: Shows the measured fit to the data, and is consistent with the fit in Figure 4.

Figures 7 shows a series of panels, each at yearly intervals. Panels 1986, 1987 and 1988 show Venus and Jupiter on the far side of the Sun from the Earth. This orientation acts to increase the effective mass of the Sun and thus the nuclear count rate increases producing the first peak. In Figure 9 panels 1997, 1998 and 1999 the orbits of Venus and Jupiter repeat producing the second peak. In between the peaks, as shown in Figure 8, Jupiter's position reduces the effective mass of the Sun thus reducing the Gravitational effect

on the Earth.
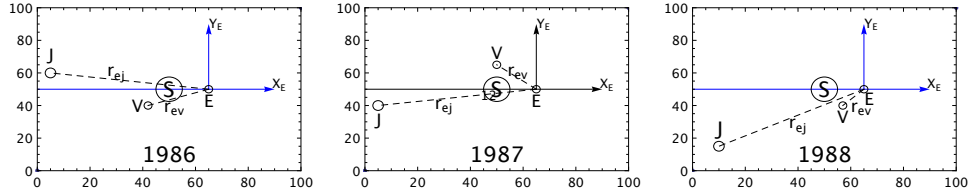


Figure 7: Each panel shows the orientation of the Planets near the first peak for years 1986 to 1988.
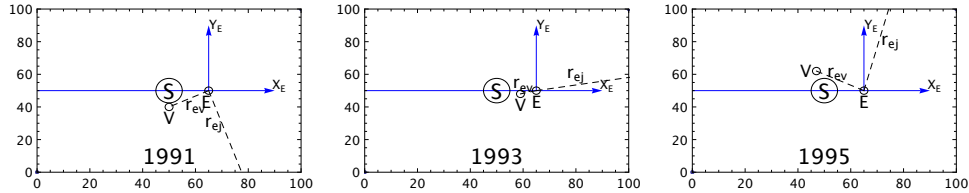


Figure 8: Selected panels where Jupiter in opposition, thus reducing the gravitation from the Sun, years 1989 to 1995.
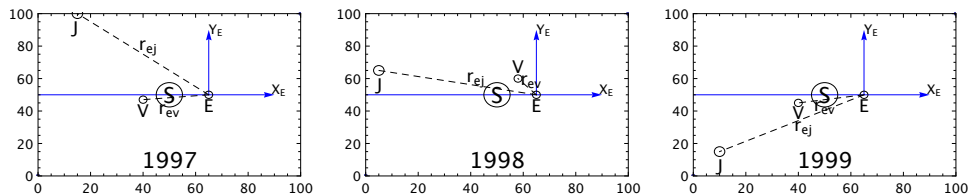


Figure 9: Panel showing the repeat orientation aligning with the gravity of the Sun. For years 1997 to 1999.

Furthermore, if gravity is the cause, one would expect the moon to have a measurable effect. The Moon is clearly shown to have an effect, as seen in [16], which shows an accumulation of 87 cycles of synodical lunar month average of the decay measurements of $^{90}Sr - ^{90}Y$. The Moon data shown by A.G.Parkhomov in his Fig 2 is consistent with the planetary effect, since the peak in the decay rate occurs at New-Moon where the Moons position reenforce the effect of the Sun, whereas at Full-Moon the decay rate in min-

16

imum and its position opposes the effect of the Sun.

## 4    Discussion

The model developed in Part I was intended to test the hypothesis that the two theories, General Relativity and Quantum Mechanics, as well as all Newtonian physics, were built on different geometric foundations thus their incoherence. A $\sigma$ field was envisioned as a way to transform coordinate variables of Newtonian Euclidian geometry to coordinate variables in the Einstein's Riemann geometry, thereby linking quantum and Newtonian physics to General Relativity. A major benefit of this approach is that neither GR or QM theory had to be modified. The present paradigm holds that the concepts of fields are abstract entities and not directly accessible. It further holds that General Relativity is the spacetime that best describes the material world. This model suggests that Newtonian and quantum physics are built in a space time that does not exist. The envisioned $\sigma$ field builds a bridge between the two geometries and links together the physics built in each. The test of the hypothesis, for which the model was built, is supported by providing an alternate explanation of the unexplained nuclear decay observations.

In Part II, as a test the model is applied to the unexplained phenomena of yearly oscillations observed in nuclear radioactive decay. The main result shows that the planetary orbits, mainly of Venus and Jupiter, explained the main features of the long run data obtain by PTB. The two main features of the PTB data matches the closely repeating planetary cycles. The Earth's moon also has an effect but was not included in the analysis due to the poor resolution of the PTB data. The moon's effect has been reported and was discussed in [16]. The observed shift of the decay data from the perihelion of the Earth is explained by the conversion from coordinate time, used in all experiments and astronomical observations, to proper time used in the analysis.

Another unexplained daily oscillation has been observed in electrochemical transmutation experiments (ECT)[18], in this case the distance from the Sun varies daily as the Earth rotates. These experiments were run for only about 450 hours and daily oscillation show a modulation that suggests the moon's participation, as expected by the model.

Table 1 provides a few dates before and after the events studied in the paper, where Venus and Jupiter support the pull of the Sun as shown in Figure 7.

The difference is that the Earth is not at a fixed position in its orbit.

Table 1: Approximate dates of possible events

| Year | Month | Year | Month |
|------|-------|------|-------|
| 1962 | 3 | 1971 | 7 |
| 1985 | 5 | 1999 | 2 |
| 2006 | 7 | 2007 | 6 |
| 2015 | 8 | 2017 | 11 |
| 2018 | 11 | 2019 | 12 |
| 2021 | 1 | 2022 | 3 |
| 2024 | 6 | 2028 | 9 |

Experiments that do not show a oscillation in the results include [19] the experiments performed at the INFI Gran Sasso Underground Laboratory. The decay experiment was located 1400 meters underground and started on June 6, 2011. The planets are aligned to produce an effect, however no oscillation was observed. The potential at the surface of the Earth, due to the planets, is $2.04 \times 10^{-6}$ $m^2/s^2$. The potential due to the Earth at the underground experiment is potential at the surface of the Earth minus the potential at the experiment due to the Earth from the center to the experiment, or $2.74 \times 10^4$ $m^2/s^2$. This implies that the signal from the planets will be attenuated by $10^8$ %, which perhaps explains the null result. Another negative result was a test to look for oscillation in a space experiment [15] analyzed the Cassini space craft RTG power source over a two year period and found no effect. The major difference between the Cassini data and the other observation is the shielding effect of the Earth's atmosphere, since $X - rays$ and $\gamma - rays$ will not penetrate the Earths atmosphere. In space the x-ray intensity, measured by the GOES-11 satellite [13] ranged from $10^{-6}$ to $10^{-7}$ $W/m^2$ over the two year test. These emissions may have mask the weak gravitational effect. Also, the RTG source is an alpha emitter that may not show the oscillation effect, see the tables in both [8] and [16].

More recently a correlation may have been observed between nuclear decay rate and the LIGO and Virgo gravitational wave detectors of the event GW170817 binary neutron star in spiral [20]. It must be noted at August 17, 2017 Venus and Jupiter orientations support the pull from the Sun however, the very narrow window of correlation does support the gravitational wave argument. If gravitation affects quantum systems as the model suggests, then it is reasonable that measurements of quantum systems would respond to gravitational waves. If true, this could open a new observational

capability for viewing the universe.

# 5    Acknowledgements

# 6    References

[1] H. Minkowski, 1908, Dover publications, 1923;
[2] C. W. Misner, K. S. Thorne, J.A. Wheeler, 1970, Gravitation;
[3] F. J. Dyson, qpt, physics.harvard.edu/Dyson-Maxwell.pdf;
[4] S. Weinberg, Gravitation and Cosmology 1972, John Wiley & Sons;
[5] R. T. Longo, viXra:1405.0244.v2, [History and Philosophy of Physics],2014;
[6] S. A.Paston, , A. A. Sheykin, , (Feb. 6, 2012). arXiv:1202.1204v1;
[7] J. R. Goodwin et al.  https://cyclotron.tamu.edu/.../2007...;
[8] D. O'keefe, et al. arXiv:1212.2198v1 [astro-ph.SR] 10 Dec 2012;
[9] J. H. Jenkins, et al. 2008, arXiv:0808.3283v1 [astro-ph] 25 Aug 2008;
[10] D. E. Alburger, et al. Earth and Planet. Sci. Lett. 78, 168 (1986);
[11] H. Siegert et al. Appl. Radiat. Isot. 49, 1397 (1998);
[12] J. H. Jenkins, E. Fischbach, arXiv: 08083156 [astro-ph] 22 Aug 2008;
[13] NOAA/NWS Space Weather Pred. Ctr., http://www.sec.noaa.gov;
[14] E. B. Norman, et al. arXiv:0810.3265 [astro-ph] 17 Oct 2008;
[15] P. S. Cooper, arXiv:0809.4248v1 [astro-ph] 24 Sep 2008;
[16] A. G. Parkhomov, arXiv:1012.4174 [physics.gen-ph] 19 Dec 2010;
[17] (SkySafari6 Pro), Apple AppStore;
[18] F. Scholkmann et al. J. Condensed Matter Nucl. Sci. 8, (2012) 37;
[19] E. Bellotti, arXiv:1202.3662v1 [nucl-ex] 16 Feb 2012;
[20] E. Fischbach, et al. arXiv:1801.03585v4 [astro-ph.HE] 21 Jun 2018;